

# Soft Matter

Accepted Manuscript



This is an *Accepted Manuscript*, which has been through the Royal Society of Chemistry peer review process and has been accepted for publication.

*Accepted Manuscripts* are published online shortly after acceptance, before technical editing, formatting and proof reading. Using this free service, authors can make their results available to the community, in citable form, before we publish the edited article. We will replace this *Accepted Manuscript* with the edited and formatted *Advance Article* as soon as it is available.

You can find more information about *Accepted Manuscripts* in the [Information for Authors](#).

Please note that technical editing may introduce minor changes to the text and/or graphics, which may alter content. The journal's standard [Terms & Conditions](#) and the [Ethical guidelines](#) still apply. In no event shall the Royal Society of Chemistry be held responsible for any errors or omissions in this *Accepted Manuscript* or any consequences arising from the use of any information it contains.

Cite this: DOI: 10.1039/xxxxxxxxxx

## Inherent structure energy is a good indicator of molecular mobility in glasses

Julian Helfferich,<sup>\*a</sup> Ivan Lyubimov,<sup>a‡</sup> Daniel Reid,<sup>a‡</sup> and Juan J. de Pablo<sup>a</sup>Received Date  
Accepted Date

DOI: 10.1039/xxxxxxxxxx

www.rsc.org/journalname

Glasses produced via physical vapor deposition can display greater kinetic stability and lower enthalpy than glasses prepared by liquid cooling. While the reduced enthalpy has often been used as a measure of the stability, it is not obvious whether dynamic measures of stability provide the same view. Here, we study dynamics in vapor-deposited and liquid-cooled glass films using molecular simulations of a bead-spring polymer model as well as a Lennard-Jones binary mixture in two and three dimensions. We confirm that the dynamics in vapor-deposited glasses is indeed slower than in ordinary glasses. We further show that the inherent structure energy is a good reporter of local dynamics, and that aged systems and glasses prepared by cooling at progressively slower rates exhibit the same behavior as vapor-deposited materials when they both have the same inherent structure energy. These findings suggest that the stability inferred from measurements of the energy is also manifested in dynamic observables, and they strengthen the view that vapor deposition processes provide an effective strategy for creation of stable glasses.

### 1 Introduction

Ordinary glasses are typically prepared by cooling a liquid at a rate that is sufficiently fast to avoid crystallization. Upon cooling towards the glass transition temperature  $T_g$ , the viscosity and characteristic relaxation times increase considerably<sup>1–5</sup>. Eventually, such relaxation times exceed the cooling rate, leading to dynamic arrest and glass formation<sup>3–5</sup>. This transition is accompanied by a change in the specific heat and defines the calorimetric glass transition temperature<sup>2,4</sup>. As the relaxation times become larger than the available laboratory time scales, the system is no longer able to reach its equilibrium state and thus “falls out of equilibrium”<sup>5</sup>. However, dynamics do not come to a halt in the glass phase. Instead, the system slowly evolves towards its equilibrium state in a process called “physical aging”, characterized by an increase of the density and the structural relaxation time<sup>6</sup>. Thus, within the traditional view of glass formation, two strategies can be followed to prepare a glass that is closer to its equilibrium state: employing a slower cooling rate, or letting the system age for an extended period of time.

Recent experiments have shown that glasses can also be created through a process of physical vapor deposition (PVD), leading to materials whose macroscopic characteristics, such as mechanical properties or onset temperature, can exceed those of highly aged ordinary glasses. Specifically, PVD glasses can ex-

hibit extraordinary thermodynamic and kinetic stability<sup>7,8</sup>, an increased density<sup>7–9</sup> and a reduced enthalpy<sup>10–13</sup>. A growing body of numerical simulations has sought to interpret from a molecular perspective available experimental observations on PVD glasses. Simulations have been able to reproduce several experimentally observed features, including higher thermodynamic and kinetic stability, the existence of an optimal substrate temperature for vapor deposition, the existence of a mobile layer at the vacuum interface, and the ability to control anisotropy through the deposition process experiments<sup>14–18</sup>.

The term “stability” is used to describe an array of properties, including a high onset temperature<sup>7</sup>, reduced bulk diffusivity<sup>7</sup>, and suppressed  $\beta$ -relaxations<sup>24</sup>. In both experimental and simulation studies, the enthalpy has been used as a convenient, easily accessible measure for the stability. In experiments, the enthalpy is typically determined by relying on calorimetry measurements<sup>11–13,19,20</sup>. In simulations, one can determine directly the average potential energy per particle and use that to assess stability<sup>15–17</sup>. The enthalpy of a PVD glass can be compared to the measured or extrapolated enthalpy of an ordinary glass that has been aged over a long period of time, thereby providing an indirect means of assessing the age and stability of a material. Such a measure of stability, however, is purely thermodynamic. It is therefore of interest to determine whether dynamic measures of stability, such as characteristic relaxation times, provide the same view of PVD glasses that, up to now, has been generated on the basis of largely thermodynamic quantities. Annealing experiments have demonstrated that, upon heating, stable glasses take a much

<sup>a</sup> Institute for Molecular Engineering, University of Chicago, 5640 South Ellis Avenue, Chicago, IL 60637, USA. E-mail: jhelfferich@uchicago.edu

‡ These authors contributed equally to this work

longer time to reach the liquid state than ordinary glasses, thereby suggesting that they exhibit strongly reduced dynamics<sup>21–23</sup>. Furthermore, dielectric measurements reveal a strong suppression of the  $\beta$ -relaxation in stable glasses<sup>24</sup>. Similar techniques, however, have not been applied in simulations of vapor-deposited glasses. Here, a connection between the inherent structure energy and the dynamics is of particular interest as the energy, similar to the enthalpy, is easily accessible, whereas long and demanding simulation runs are necessary to extract dynamic properties.

More generally, in this work we address the issue of whether vapor deposited glasses are dynamically equivalent to aged glasses. We examine whether the dynamics in vapor deposited glasses are comparable to those of glasses aged over long periods of time. We ask if vapor deposited glasses are indeed closer to the equilibrium state than ordinary glasses, or if they represent a “hidden amorphous state”<sup>25</sup> that transforms back to an ordinary glass over time.

To approach these questions, we analyze the decay of the incoherent intermediate scattering function (ISF) in vapor deposited and ordinary glasses for three different glass formers: a bead-spring polymer melt, a two-dimensional binary mixture, and a three-dimensional binary mixture. For all three systems, we find that the dynamics are indeed strongly slowed in stable glasses. Furthermore, we confirm that none of the models considered here displays any sign of a “hidden amorphous state”. Instead, we find that the inherent structure energy is a good indicator for the dynamics, and that slowly cooled or aged ordinary glasses with the same inherent structure energy as a vapor deposited glass display almost identical dynamics. This finding also holds for vapor deposited and liquid cooled polymer films, which are structurally different.

Our manuscript begins with a summary of the simulation techniques employed in this work (Sec. 2), followed a discussion of the corresponding results (Sec. 3). We conclude with general remarks pertaining to the stability and anisotropy of vapor deposited glasses (Sec. 4).

## 2 Methods

The models and simulation protocols used to replicate the vapor deposition process have been described in the literature for the polymer system<sup>17</sup>, the 3D Lennard-Jones binary mixture (3dBm)<sup>15,16</sup>, and the 2D Lennard-Jones binary system (2dBm)<sup>26</sup>. For completeness, only a brief summary is provided in what follows. The first glass former we consider is a binary mixture consisting of two types of particles, type *A* and type *B*, in a ratio of 80/20 for the 3dBm system and 65/35 for the 2dBm system<sup>27</sup>. The particles interact via a Lennard-Jones (LJ) potential truncated at  $r_{\text{trunc}} = 2.4$  and extrapolated to smoothly decay to zero at  $r_c = 2.5$ . In the following, all values are reported in LJ units. To this end, we set  $\epsilon_{AA} = 1$ ,  $\sigma_{AA} = 1$ , the mass  $m = 1$ , and  $k_B = 1$ . In these units, the relevant interaction parameters are  $\epsilon_{AB} = 1.5$ ,  $\sigma_{AB} = 0.8$ ,  $\epsilon_{BB} = 0.5$ , and  $\sigma_{BB} = 0.88$ .

As an alternative glass former, we study a simple bead-spring polymer model. The polymer system consists only of type-*A* particles, connected via bonds to form chains of length  $N = 4$  or  $N = 10$ , well below the entanglement length<sup>28</sup>. Bonded particles (beads)

	Polymer $N = 4$			Binary mixture (3d)			
$T$	0.3	0.35	0.4	0.275	0.3	0.325	0.35
$T/T_g$	0.79	0.92	1.05	0.79	0.86	0.93	1.00
	Polymer $N = 10$			Binary mixture (2d)			
$T$	0.3	0.35	0.4	0.166	0.182	0.193	0.221
$T/T_g$	0.73	0.85	0.98	0.79	0.87	0.92	1.05

**Table 1** Temperatures at which the ISF is determined

are connected by a harmonic potential, whose spring constant  $K = 1000$  and equilibrium bond length  $l_0 = 0.97$  are chosen to prevent chain crossings and inhibit crystallization<sup>29</sup>. The substrate consists of a third type of atoms. It interacts with the glass former via a LJ potential with the following interaction parameters:  $\epsilon_{AS} = \epsilon_{BS} = 0.1$  (3d BM),  $\epsilon_{AS} = \epsilon_{BS} = 1.0$  (2d BM, polymer),  $\sigma_{AS} = 0.75$  (2d/3d BM),  $\sigma_{AS} = 1.0$  (polymer),  $\sigma_{BS} = 0.7$  (3d BM),  $\sigma_{BS} = 0.75$  (2d BM),  $\epsilon_{SS} = 0.1$ , and  $\sigma_{SS} = 0.6$ .

To replicate the vapor deposition process, we first place  $N_s$  substrate atoms randomly in a thin layer at the bottom of the simulation box and minimize the energy to remove overlap and to spread the atoms evenly across the layer. Then, the substrate atoms are tethered to their current position using a harmonic spring with spring constant  $K = 1000$ . Onto this substrate we deposit the glass former. For the polymer glass and the 3dBm system, we iterate the following steps: (1) We introduce either a set of 10 particles of the binary mixture or one polymer chain into the system and bring it into contact with the surface of the film (or the substrate if no film has yet formed); (2) We slowly cool the newly introduced particle(s) to the substrate temperature; and (3) We perform energy minimization using the FIRE algorithm<sup>30</sup>. These steps are designed to improve the efficiency of the simulation by assisting the newly deposited particle(s) in finding their most favorable, nearby local energy minimum. During deposition and the subsequent isothermal run, all particles are coupled to an external heat bath using the Nosé-Hoover thermostat<sup>31,32</sup>. This procedure differs from the experimental situation in that local equilibrium is attained by quenching the system to a nearby energy minimum through a steepest-descent procedure. By taking advantage of the reduced numerical complexity afforded in two dimensions, for the 2dBm system we follow a more realistic algorithm in which only the substrate atoms are coupled to an external heat bath, and we refrain from performing energy minimizations. Instead, we allow newly deposited particles to reach the equilibrium (substrate) temperature through “natural” energy dissipation mechanisms.

After the deposition is complete, all films are relaxed for 500 LJ-time units before collecting data. Ordinary glass films are created by heating vapor deposited films well above the glass transition temperature and slowly cooling them to the desired temperature at a specified cooling rate.

In order to study the microscopic dynamics, we deposited films at various substrate temperatures in the range from  $0.73T_g$  to  $1.05T_g$  (see Table 1). At each temperature, we perform isothermal runs on four independent configurations for each system.

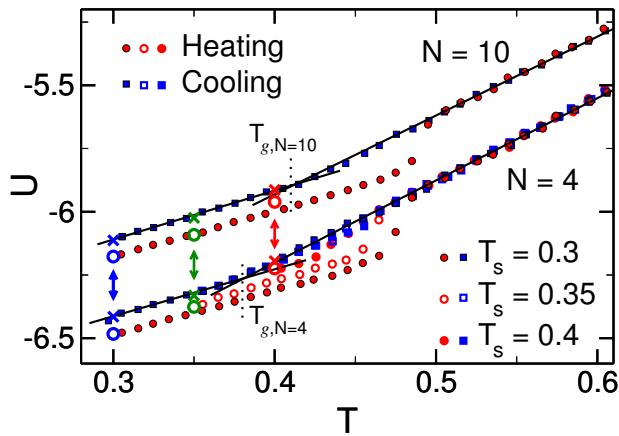


**Fig. 1** Average potential energy per particle,  $U$ , for the polymer model with chains of length  $N = 4$  and  $N = 10$  during a heating run from  $T_s$  to  $T = 0.8$  (circles) and a subsequent cooling run back to  $T_s$  (squares). For both systems, the heating/cooling rate is  $q_c = 10^{-5}$ . For  $N = 4$ , the potential energy for systems deposited at  $T_s = 0.3$  (solid symbols),  $T_s = 0.35$  (open symbols), and  $T_s = 0.4$  (hatched symbols) are displayed. For  $N = 10$  only the potential energy for the system deposited at  $T_s = 0.3$  is displayed. The potential energy has been averaged over all particles in the center region of the film and the results for  $N = 10$  have been shifted by 0.2 for clarity. The solid lines are fits to the linear regimes, the vertical lines indicate the values of  $T_g$  as defined in the main text. The arrows indicate the temperatures at which the ISF is calculated and the circles and crosses mark the potential energy at the start of the calculation for vapor deposited and ordinary glasses, respectively.

### 3 Results and discussion

We begin our discussion with an analysis of our results for the polymer model. In order to compare vapor deposited glasses to ordinary glasses, vapor deposited materials are heated to  $T = 0.8$ , well above the glass transition temperature, and cooled back down to the desired temperature at a rate of  $q_c = 10^{-5}$ . During this heating/cooling run, we calculate the average potential energy in the center region of the film<sup>17</sup>. Our aim is to reproduce standard differential scanning calorimetry procedures, albeit at much higher cooling rates than those typically used in experiments. Our results for the energy, shown in Fig. 1, bear several of the characteristics that have been experimentally observed in stable glasses: A lower potential energy, and an onset temperature  $T_{\text{on}}$  that is much higher than the glass transition temperature  $T_g$  for the same cooling/heating rate. These findings have been reported elsewhere, and strongly indicate that vapor-deposited materials lie deeper in the potential energy landscape<sup>17</sup>. What has perhaps not been firmly established before, however, is whether a low potential energy does indeed translate into slower structural relaxation in vapor deposited materials.

Our analysis of dynamics is performed by relying on the glass transition temperature as a reference. In this work, we use the simulated potential energy curves to define the relevant simulated glass transition temperatures  $T_g$  by identifying two linear regimes in the cooling run, one corresponding to the equilibrium supercooled liquid and another to the glass regime, respectively. We then fit the data in the linear regimes (solid lines in Fig. 1) and calculate the intersection point. For the polymer systems consid-

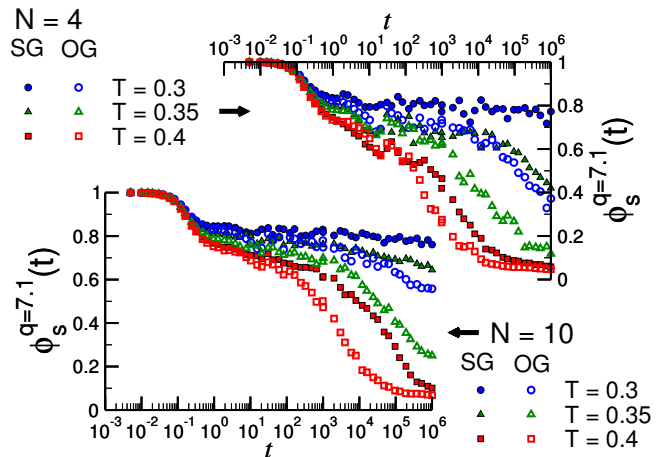


**Fig. 2** ISF  $\phi_s^q(t)$  for chains of length  $N = 4$  (top panel) and  $N = 10$  (bottom panel). The solid symbols represent the results for the stable glass (SG), the open symbols those for the ordinary glass (OG). The ISF is determined at temperatures  $T = 0.3$  ( $\circ$ ),  $0.35$  ( $\Delta$ ), and  $0.4$  ( $\square$ ).

ered here, we find  $T_g = 0.38$  for  $N = 4$  and  $T_g = 0.41$  for  $N = 10$ . For the binary systems, we find  $T_g = 0.35$  in three dimensions<sup>16</sup> and  $T_g = 0.21$  in the two-dimensional model<sup>26</sup>.

The incoherent intermediate scattering function (ISF) is given by

$$\phi_s^q(t, t_a) = \frac{1}{N} \sum_{k=1}^N \langle \exp[i\mathbf{q} \cdot (r_k(t_a + t) - r_k(t_a))] \rangle, \quad (1)$$

where  $t_a$  is the aging time, i.e. the time between the start of the trajectory and the start of the measurement, and the average  $\langle \cdot \rangle$  is taken over 200  $\mathbf{q}$ -vectors in random directions. Here,  $|\mathbf{q}|$  corresponds to the first peak in the static structure factor, which is at  $|\mathbf{q}| = 0.71$  for the polymer melt, 0.721 for the 3dBm system, and 0.59 for the 2dBm system. For simplicity, we use  $\phi_s^q(t, t_a = 0) \equiv \phi_s^q(t)$ .

Our results for the polymer system are shown in Fig. 2. First, we note that our basic hypothesis holds true: the decay of the ISF for vapor-deposited materials is slower than for their ordinary counterparts, indicating that the dynamics of simulated vapor-deposited glasses are significantly slower. This observation holds for all temperatures and both chain lengths. Furthermore, we note that the plateau value is slightly larger for the vapor deposited glass compared to the respective liquid-cooled one. This observation is consistent with the increased density observed in vapor-deposited systems. It is important to emphasize that, at least for the  $N = 10$  polymeric system, the structure of vapor deposited glasses is highly anisotropic and considerably different from that of the corresponding ordinary material<sup>17</sup>. As such, it is particularly important to stress that for these materials, a lower potential energy continues to correspond to slower dynamics, even if the material adopts different molecular packing arrangements. This finding is also relevant in view of recent findings, which indicate that vapor-deposition enables control of molecular anisotropy in stable glasses<sup>8,33,34</sup>.

We further note that dynamics in the vapor deposited glass is significantly slower than in the ordinary material, even when deposited above  $T_g$ , as can be seen in Fig. 2 for chains of length

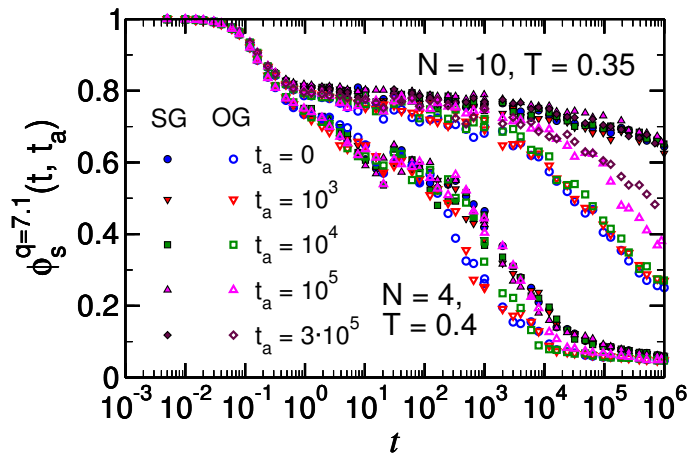


**Fig. 3** ISF  $\phi_s^q(t, t_a)$  for chains of length  $N = 4$  at  $T = 0.4$  and  $N = 10$  at  $T = 0.35$ . The ISFs are calculated both for the stable glass (SG, solid symbols) and the ordinary glass (OG, open symbols) at various aging times  $t_a = 0$  ( $\circ$ ),  $10^3$  ( $\nabla$ ),  $10^4$  ( $\square$ ), and  $10^5$  ( $\triangle$ ), as well as  $t_a = 3 \cdot 10^5$  ( $\diamond$ ) for chain of length  $N = 10$ .

$N = 4$  (deposited at  $T = 0.4$ ). Given the fact that the potential energy at  $T = 0.4$  is very close to the equilibrium supercooled-liquid line, the question arises as to which of the two systems corresponds to the equilibrium state. To address this issue, we calculate the ISF for various aging times. Figure 3 shows results for  $N = 4$  at  $T = 0.4$  and  $N = 10$  at  $T = 0.35$ . First, we note that at  $T = 0.4$ , the vapor deposited glass is in equilibrium, whereas for the fast cooling rates considered here, the system cooled from the liquid state retains some memory from its process of formation. We attribute this behavior to the polymeric nature of the molecules: while the system is able to relax on the scale of the individual chain segments at  $T = 0.4$ , it is not able to do so on the length scale of the entire chains. Our observation is further supported by the fact that the short chains deposited at  $T = 0.4$  show an onset temperature slightly larger than the glass transition temperature (see Fig. 1). For the longer chains  $N = 10$ , below  $T_g$  equilibrium can no longer be attained by aging on the time scales considered here. Instead, we observe the typical aging behavior in which the plateau value increases and the decay from the plateau shifts to later times. In contrast, for the vapor deposited material, we find no evidence of aging on the time scales accessible to our simulations: the ISF data remain unchanged for all aging times studied in this work. Given that the potential energy of the stable glass lies on the extrapolated supercooled liquid line, it is plausible to assume that the system has reached its equilibrium potential energy. This observation further underscores that vapor deposition provides a surprisingly effective experimental and simulation technique for preparation of glasses whose properties are difficult to attain via traditional liquid-cooling processes.

We now consider whether the 3D and 2D binary mixtures prepared by vapor deposition also exhibit slower dynamics. The ISFs for the 3-dimensional system are shown in Fig. 4. First, we note that the general behavior is similar to that found for the polymer system, albeit the difference between ordinary and stable glasses is less pronounced. As with the polymers, the difference in dynamics between the vapor deposited and the ordinary glass in-

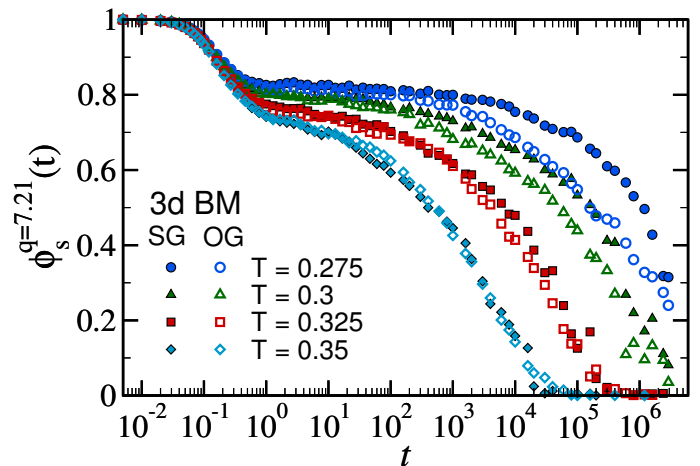


**Fig. 4** ISF  $\phi_s^q(t)$  for 3d binary mixture stable glass (SG, full symbols) and ordinary glass (OG, open symbols) films at four different temperatures:  $T = 0.275$  ( $\circ$ ),  $0.3$  ( $\triangle$ ),  $0.325$  ( $\square$ ), and  $0.350$  ( $\diamond$ ).

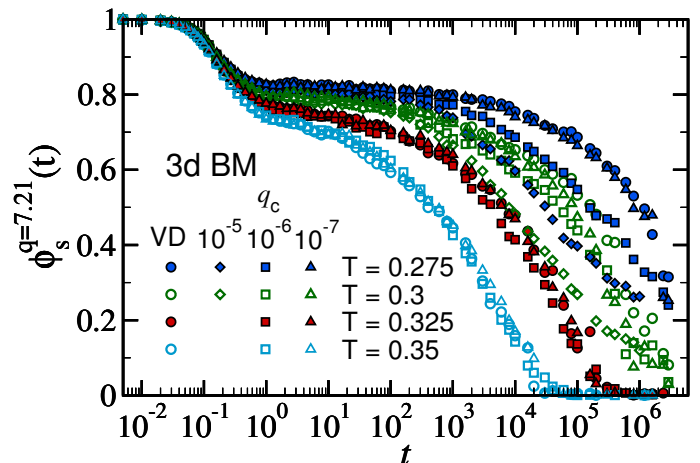


**Fig. 5** ISF  $\phi_s^q(t)$  for 3d binary mixture of a vapor deposited glass (VD,  $\circ$ ) and ordinary glasses formed using three different cooling rates  $q_c = 10^{-5}$  ( $\triangle$ , shown only for the two lowest temperatures),  $10^{-6}$  ( $\square$ ), and  $10^{-7}$  ( $\diamond$ ). The films were deposited at or cooled to four different temperatures:  $T = 0.275$ ,  $0.3$ ,  $0.325$ , and  $0.350$ .

creases with lower deposition temperatures.

For the polymer systems we examined the effect of aging on the material. For the LJ mixtures, we examine the effect of cooling rate. Specifically, we consider the following three rates  $q_c = 10^{-5}$ ,  $10^{-6}$ , and  $10^{-7}$ . The corresponding ISFs are displayed in Fig. 5. As expected, the dynamics are markedly slower for systems cooled by slower cooling rates. For the slowest cooling rate considered here, the dynamics almost overlap with those of the as-deposited films. We note, however, that the liquid-cooling procedure is much more computationally demanding than vapor deposition.

These results do, in fact, raise a more fundamental question: What is a fair comparison between vapor deposited and liquid cooled films? This question is particularly important for numerical simulations, where typical cooling rates are orders of magnitude faster than the  $1 \text{ K/min}$  typically employed in experiments. Two measures can be considered: One can (1) compare cooling

$T$	0.166	0.182	0.193	0.221
$U_{\text{VD}}^{\text{IS}}$	-3.719	-3.710	-3.704	-3.686
$U_{\text{c2}}^{\text{IS}}$	-3.719	-3.716	-3.701	-3.688
$U_{\text{c1}}^{\text{IS}}$	-3.716	-3.708	-3.696	-3.690

**Table 2** Inherent structure energy  $U^{\text{IS}}$  for the vapor deposited film (VD) and two liquid-cooled films using the cooling rates  $q_{\text{c2}} = 2 \cdot 10^{-7}$  and  $q_{\text{c1}} = 1.33 \cdot 10^{-6}$ . The cooling rates are chosen such that (1) the cooling time is identical to the deposition time or (2) the inherent structure energy of vapor deposited and liquid cooled films are approximately equal.

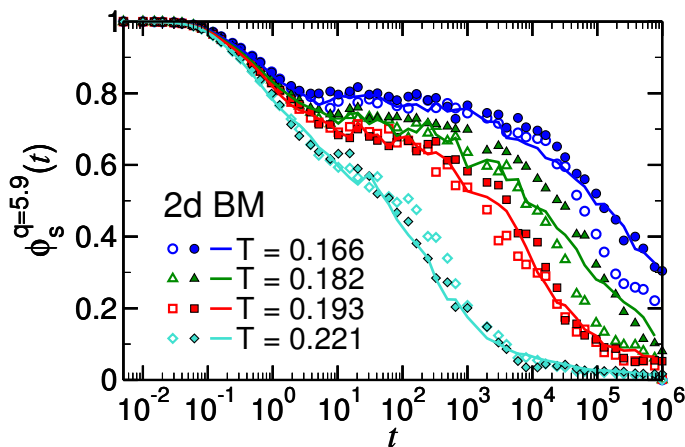


**Fig. 6** ISF  $\phi_s^q(t)$  for a 2d binary mixture of a vapor deposited glass (lines) and two ordinary glasses formed using two different cooling rates  $q_c$ . The cooling rates were chosen such that the ordinary glass forms in the same amount of time as the vapor deposited one (open symbols,  $q_c = 1.33 \cdot 10^{-6}$ ) or such that both films obtain the same inherent structure energy (solid symbols,  $q_c = 2 \cdot 10^{-7}$ ). The glasses were deposited at or cooled to four temperatures  $T = 0.166$  ( $\circ$ ),  $0.182$  ( $\Delta$ ),  $0.325$  ( $\square$ ), and  $0.350$  ( $\diamond$ ).

and deposition protocols that are run over the same amount of time, measured in LJ time units, or, (2), which processes lead to the same inherent structure energy, i.e. which glasses are comparable in terms of the potential energy landscape. The lowest inherent structure energies that can be reached by vapor deposition are, in general, not attainable by liquid cooling. To reach the lowest inherent structure energy reported in Ref. <sup>26</sup> by liquid cooling, a rate on the order of  $10^{-13}$  would be necessary, requiring on the order of thousands of years of simulation time on a typical CPU. For the purposes of this manuscript, we have thus deliberately chosen suboptimal parameters for the vapor deposition process, leading to rather "poor" glasses in comparison. Only these suboptimal parameters allow the liquid cooled system to reach in reasonable timescales the same inherent structure energy that is achieved by vapor deposition. The inherent structure energies for the three different protocols are listed in Table 2. We note that the inherent structure energies are lower for the vapor deposited films compared to the liquid cooled ones formed during the same amount of time, except for the highest temperature which is above  $T_g$ . This demonstrates that vapor deposited glass lie deep in the potential energy landscape.

The ISFs for the three different formation protocols are dis-

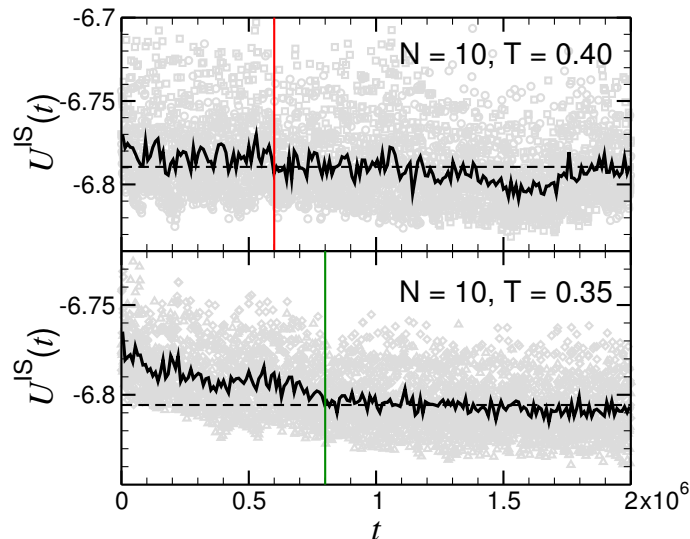


**Fig. 7** Inherent structure energy  $U^{\text{IS}}(t)$  for the ordinary glass cooled to  $T = 0.40$  (upper panel) and  $0.35$  (lower panel). The solid line displays  $U^{\text{IS}}$  averaged over 20 trajectory points, 10 each from two independent configurations.  $U^{\text{IS}}$  for the individual trajectory points is displayed as grey symbols. The horizontal dashed line indicates the average inherent structure energy of the just-deposited stable glass deposited at  $T_s = 0.40$  (upper panel) and  $0.35$  (lower panel). The vertical lines indicate the times at which the ordinary glass reaches approximately the inherent structure energy of the vapor deposited glass directly after deposition.

played in Fig. 6. Two conclusions can be drawn from the figure. First, at lower temperatures, the ISF decays faster for the liquid cooled system formed over the same amount of time as the vapor deposited film. This further substantiates our premise that vapor deposition provides an efficient means by which to form glasses that reside deep in the potential energy landscape. Second, glasses that reach the same inherent structure energy via slow liquid cooling or vapor deposition exhibit almost identical dynamics. In fact, the ISFs mostly overlap with  $T = 0.182$  being a notable outlier. This is, however, not surprising given the fact that the inherent structure energy is lower for the slowly cooled system at this temperature (see Table 2). Thus, Fig. 6 suggests that systems with the same inherent structure energy display identical dynamics as measured by the incoherent scattering function. This is far from obvious, considering the different formation protocols, yet it is not implausible given that both systems are structurally almost indistinguishable (see supplementary material of Ref. <sup>26</sup>) Furthermore, a similarly strong connection between the inherent structure energy and the relaxation time has been established in polymer glasses undergoing creep deformation <sup>35,36</sup>.

To test whether this finding holds also for systems that are structurally different, we turn again to the polymer system with chains of length  $N = 10$ . During deposition, these polymers stretch out on the surface and retain their alignment as the film grows <sup>17</sup>. Thus, vapor deposited polymer films display strong anisotropy, with the end-to-end vectors of the polymers closely aligned parallel to the film surface. Liquid-cooled polymer films, on the other hand, are fully isotropic. To determine the inherent structure energy  $U^{\text{IS}}$ , we performed an isothermal run and minimized the energy at regular intervals  $\Delta t$  using the FIRE <sup>30</sup> al-

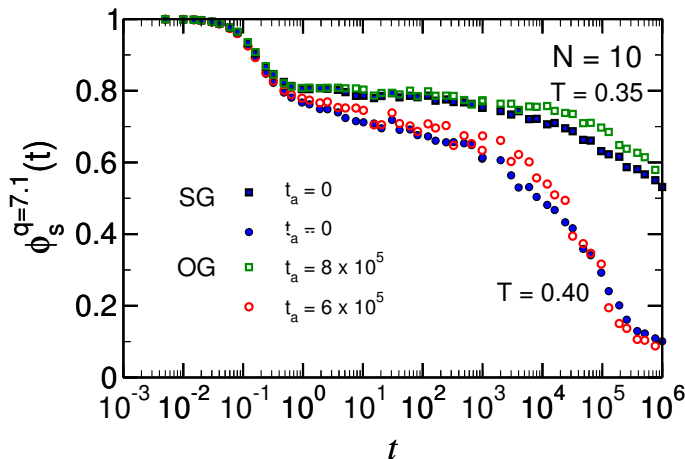


**Fig. 8** ISF  $\phi_s^q(t)$  for the vapor deposited glass (SG, solid symbols) and the ordinary glass (OG, open symbols) deposited at or cooled to  $T = 0.40$  ( $\circ$ ) and  $0.35$  ( $\square$ ). The ordinary glass was aged at  $T = 0.40$  and  $0.35$  for  $t_a = 5 \cdot 10^5$  and  $8 \cdot 10^5$ , respectively. The aging times were chosen such that both ordinary and stable glass have the same inherent structure energy (see Fig. 7).

gorithm. We determined the average  $U^{IS}$  for the vapor deposited glass within the first 1000 LJ time units ( $\Delta t = 100$ ). Next, we determined  $U^{IS}(t)$  for the ordinary glass over a long trajectory ( $\Delta t = 1000$ ) and estimated the time at which the inherent structure energy reached the same value as the just-deposited film. The results are displayed in Fig. 7. At  $T = 0.40$ , i.e. above the glass transition temperature,  $U^{IS}(t)$  changes only a little, whereas at  $T = 0.35$  a clear trend is visible. We estimate that after a time  $t_a = 6 \cdot 10^5$  for the system above  $T_g$  and  $t_a = 8 \cdot 10^5$  for the system below  $T_g$ , the ordinary glass has the same inherent structure energy as the vapor deposited glass. As for the 2d-KA system, we have again deliberately chosen suboptimal parameters for the vapor deposited glass at  $T = 0.35$ , using a deposition rate that is about one order of magnitude faster than that for all other polymer systems considered here. It is only with this very fast deposition rate that we arrive at an inherent structure energy that is sufficiently high to be attainable by simple aging of an ordinary glass.

The results for the ISF are displayed in Fig. 8. We find that the ISFs of the vapor deposited glass and the ordinary glass are essentially identical, given the fact that they exhibit the same inherent structure energy. We emphasize that this result holds regardless of the strong anisotropy of the vapor deposited film, which hardly changes over the course of the simulation run. It is important to emphasize that this does not imply that the systems are in the same state. In fact, given the structural differences, we expect them to exhibit different mechanic and thermodynamic properties, and it would not be surprising if they displayed a different aging behavior. However, our results suggest that the inherent structure energy is a good indicator to gauge the local dynamics. Thus, we infer that it is also a good measure of the stability of the glass. Furthermore, this finding can also be interpreted in terms of the potential energy landscape. The similar dynamics of the systems, despite their different structures, suggests that

they are not only in a potential that has the same depth (i.e. the same inherent structure energy), but also that the potential energy barriers surrounding them have similar heights, leading to similar dynamics. This, surprisingly, appears to hold even though pronounced structural differences indicate that the systems are in very different areas of the potential energy landscape. In other words, one could also argue that in deep energy minima, a different structure does not necessarily imply that the potential energy landscape exhibits a considerably different shape. To test whether this inference holds, i.e. whether the local properties of the potential energy landscape are indeed similar, is of high relevance and the focus of our ongoing research.

## 4 Conclusions

In this paper, we have demonstrated that the increased thermodynamic stability of simulated vapor deposited glasses is also manifest in the microscopic dynamics, as measured by the incoherent intermediate scattering function. These dynamics resemble closely those observed in ordinary glasses aged for long periods of time or liquid-cooled materials prepared at slow cooling rates. This may not come as a surprise. Indeed, vapor deposited glasses have been frequently compared to glasses aged for long times<sup>10,19</sup>. Note, however, it is not immediately obvious that vapor deposited and well-aged glasses should exhibit identical dynamics. Indeed, a contrasting hypothesis would be that a vapor deposition process puts the glass in a “stable state” that is not accessible via liquid cooling, from which the system would transform back into an ordinary glass. In fact, experiments suggest that some organic molecules are indeed deposited in a “hidden amorphous state” not accessible via liquid cooling<sup>25</sup>. However, the results presented here show no evidence for such states, neither for a bead-spring polymer model, where chains remain in an anisotropic state, nor for a binary mixture which is, by construction, fully isotropic. We have compared the ISFs of vapor-deposited glasses to those of ordinary glasses either aged for various times or cooled at different cooling rates. We find that the dynamics of ordinary glasses gradually approach those of a vapor deposited glass for longer aging times and slower cooling rates. Here we note that vapor deposition represents a very different and efficient process for preparation of well-equilibrated glasses, both in experiments and in numerical simulations. Finally, we also compared vapor deposited glasses and ordinary glasses where either the cooling rate or the aging time were adjusted such that their final states would have the same inherent structure energy. We found that these systems display the same dynamics, even when comparing a highly anisotropic vapor deposited polymer film to a structurally different, isotropic, liquid-cooled one. This finding supports the assumption that the inherent structure energy is a good measure of the stability of a glass.

## Acknowledgements

We gratefully acknowledge insightful and inspiring discussions with Mark Ediger, Jack Douglas, Francis Starr, and Wengang Zhang. JH acknowledges the financial support from the DFG research fellowship program, grant No. HE 7429/1. This work is

supported by the National Science Foundation under grant DMR-1234320.

## References

- 1 L. Berthier and G. Biroli, *Rev. Mod. Phys.*, 2011, **83**, 587.
- 2 M. D. Ediger and P. Harrowell, *J. Chem. Phys.*, 2012, **137**, 080901.
- 3 G. Biroli and J. P. Garrahan, *J. Chem. Phys.*, 2013, **138**, 12A301.
- 4 E.-J. Donth, *The Glass Transition*, Springer-Verlag, 2001.
- 5 K. Binder and W. Kob, *Glassy Materials and Disordered Solids*, World Scientific Publishing, 2011.
- 6 L. C. E. Struik, *Physical aging in amorphous polymers and other materials*, Elsevier, 1978.
- 7 S. F. Swallen, K. L. Kearns, M. K. Mapes, Y. S. Kim, R. J. McMahon, M. D. Ediger, T. Wu, L. Yu and S. Satija, *Science*, 2007, **315**, 353.
- 8 K. Ishii and H. Nakayama, *Phys. Chem. Chem. Phys.*, 2014, **16**, 12073.
- 9 S. S. Dalal and M. D. Ediger, *J. Phys. Chem. Lett.*, 2012, **3**, 1229.
- 10 K. L. Kearns, S. F. Swallen, M. D. Ediger, T. Wu, Y. Sun and L. Yu, *J. Phys. Chem. B*, 2008, **112**, 4934.
- 11 K. L. Kearns, S. F. Swallen, M. D. Ediger, Y. Sun and L. Yu, *J. Phys. Chem. B*, 2009, **113**, 1579.
- 12 E. León-Gutierrez, G. Garcia, M. T. Clavaguera-Mora and J. Rodríguez-Viejo, *Thermochim. Acta*, 2009, **492**, 51.
- 13 K. Dawson, L. Zhu, L. A. Kopff, R. J. McMahon, L. Yu and M. D. Ediger, *J. Phys. Chem. Lett.*, 2011, **2**, 2683.
- 14 S. Singh and J. J. de Pablo, *J. Chem. Phys.*, 2011, **134**, 194903.
- 15 S. Singh, M. D. Ediger and J. J. de Pablo, *Nature Materials*, 2013, **12**, 139.
- 16 I. Lyubimov, M. D. Ediger and J. J. de Pablo, *J. Chem. Phys.*, 2013, **139**, 144505.
- 17 P.-H. Lin, I. Lyubimov, L. Yu, M. D. Ediger and J. de Pablo, *J. Chem. Phys.*, 2014, **140**, 204504.
- 18 I. Lyubimov, L. Antony, D. M. Walters, D. Rodney, M. D. Ediger and J. J. de Pablo, *J. Chem. Phys.*, 2015, **143**, 094502.
- 19 K. L. Kearns, S. F. Swallen, M. D. Ediger, T. Wu and L. Yu, *J. Chem. Phys.*, 2007, **127**, 154702.
- 20 K. R. Whitaker, D. J. Scifo, M. D. Ediger, M. Ahrenberg and C. Schick, *J. Phys. Chem. B*, 2013, **117**, 12724.
- 21 Z. Chen, A. Sepulveda, M. D. Ediger and R. Richert, *J. Chem. Phys.*, 2013, **138**, 12A519.
- 22 A. Sepulveda, S. F. Swallen and M. D. Ediger, *J. Chem. Phys.*, 2013, **138**, 12A517.
- 23 A. Sepulveda, M. Tylinski, A. Guiseppi-Elie, R. Richert and M. D. Ediger, *Phys. Rev. Lett.*, 2014, **113**, 045901.
- 24 H. B. Yu, M. Tylinski, A. Guiseppi-Elie, M. D. Ediger and R. Richert, *Phys. Rev. Lett.*, 2015, **115**, 185501.
- 25 K. J. Dawson, K. L. Kearns, L. Yu, W. Steffen and M. D. Ediger, *Proc. Natl. Acad. Sci. USA*, 2009, **106**, 15165.
- 26 D. Reid, Submitted to Nature Communications.
- 27 R. Brüning, D. A. St-Onge, S. Patterson and W. Kob, *J. Phys. Condens. Matter*, 2009, **21**, 035117.
- 28 R. Everaers, S. K. Sukumaran, G. S. Grest, C. Svaneborg, A. Sivasubramanian and K. Kremer, *Science*, 2004, **303**, 823.
- 29 G. S. Grest and M. Murat, *Monte Carlo and Molecular Dynamics Simulations in Polymer Science*, Oxford University Press, 1995.
- 30 E. Bitzek, K. P., F. Gähler, M. Moseler and P. Gumbsch, *Phys. Rev. Lett.*, 2006, **97**, 170201.
- 31 W. Shinoda, M. Shiga and M. Mikami, *Phys. Rev. B*, 2004, **69**, 134103.
- 32 D. Frenkel and B. Smit, *Understanding Molecular Simulation*, Academic Press, 2002.
- 33 K. Dawson, L. A. Kopff, L. Zhu, R. J. McMahon, L. Yu, R. Richert and M. D. Ediger, *J. Chem. Phys.*, 2012, **136**, 094505.
- 34 D. Bhattacharya and V. Sadtschenko, *J. Chem. Phys.*, 2014, **141**, 094502.
- 35 R. A. Riggleman, K. S. Schweizer and J. J. de Pablo, *Macromolecules*, 2008, **41**, 4969.
- 36 R. A. Riggleman, G. N. Toepperwein, G. J. Papakonstantopoulos and J. J. de Pablo, *Macromolecules*, 2009, **42**, 3632.